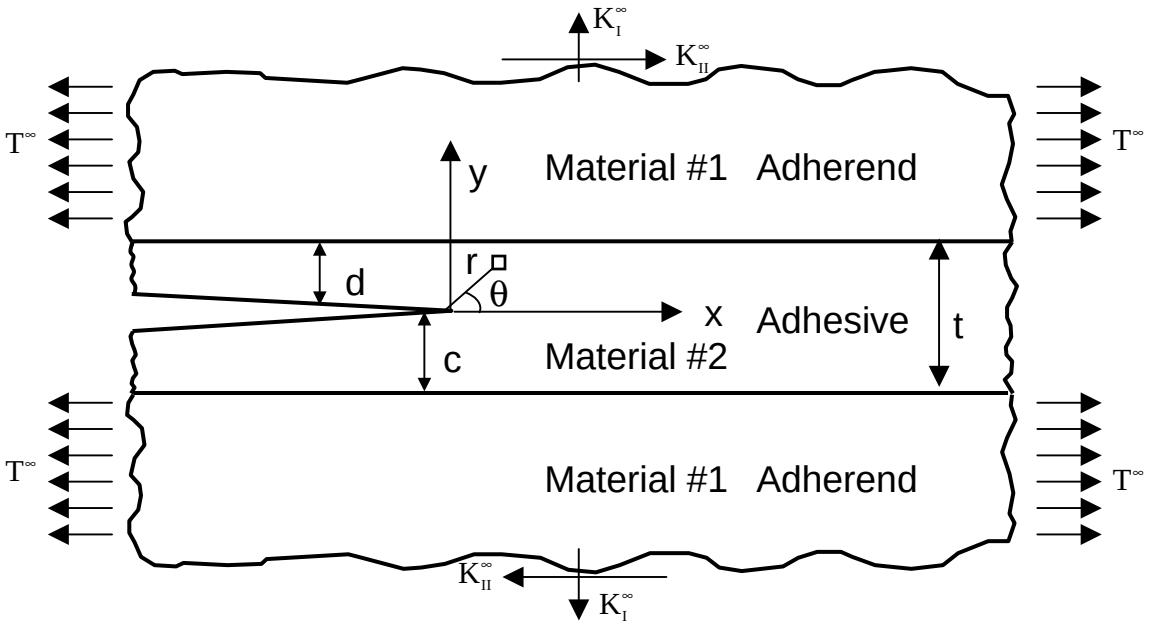

Fig. 1. A crack within the adhesive layer in an adhesive bond. The adherend is designated as material 1 and adhesive is designated as material 2. The coordinate system is set at the crack tip.

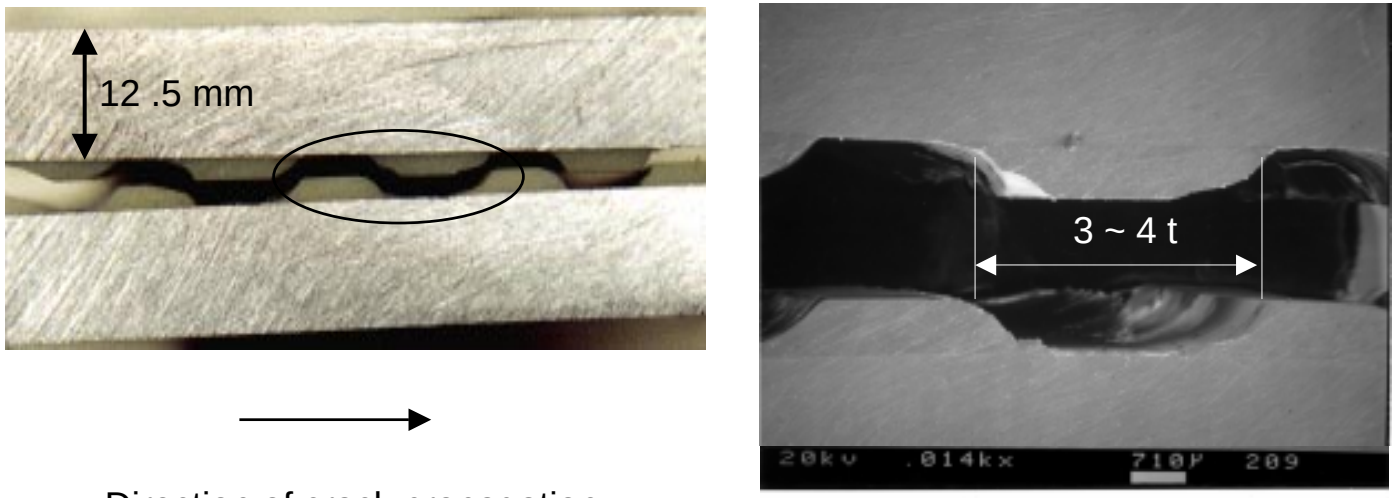

Fig. 2. The cross-section of the failed specimen with T = 35 MPa and alternating crack trajectory. The picture on the right is the scanning electron microscopy (SEM) micrograph of the circled portion of the cross-section.

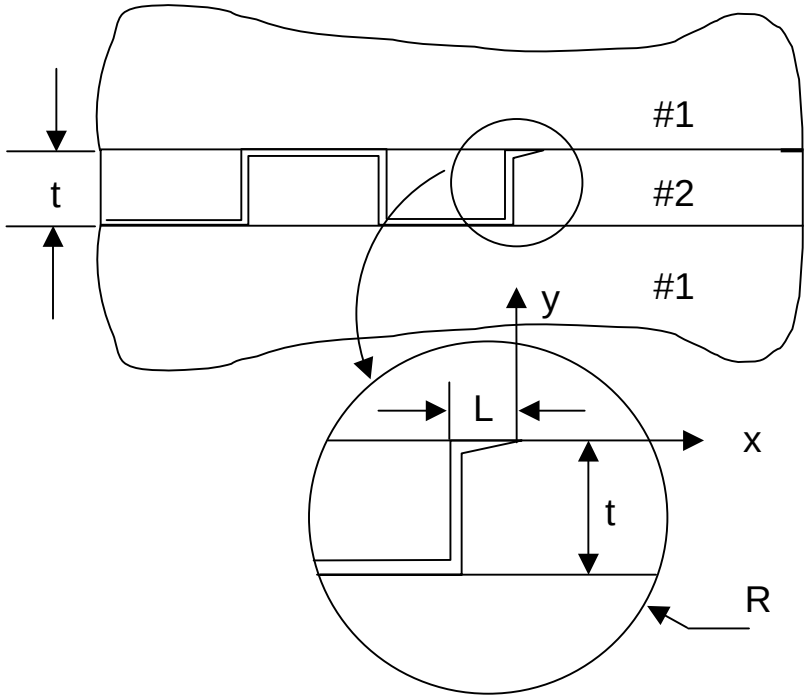

Fig. 3. The idealized crack trajectory geometry used in references 1 and 2.

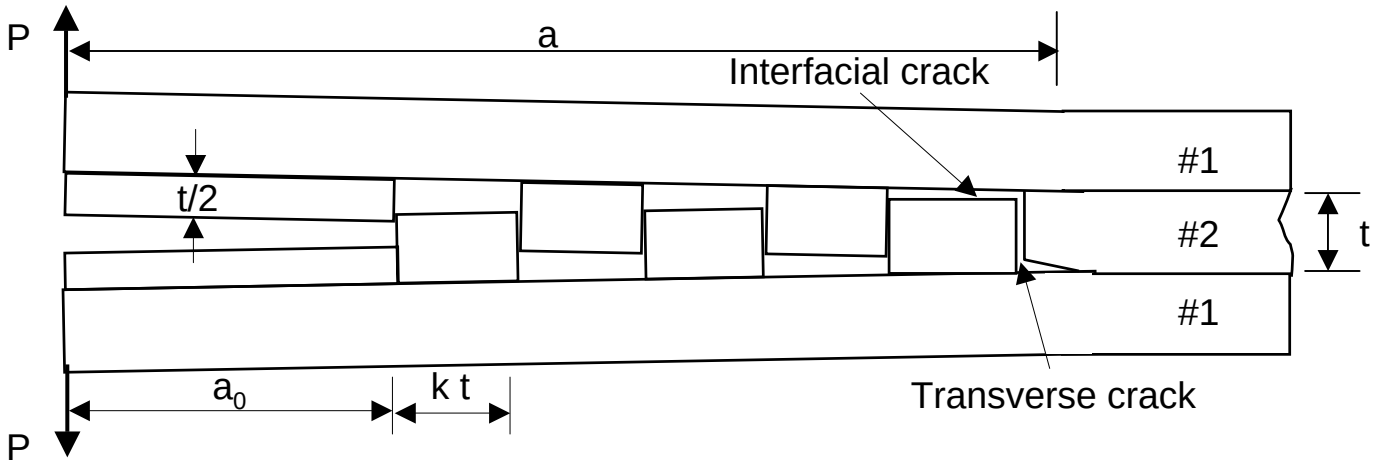

Fig. 4. A double cantilever beam (DCB) specimen with simplified crack trajectory for directionally unstable crack propagation.

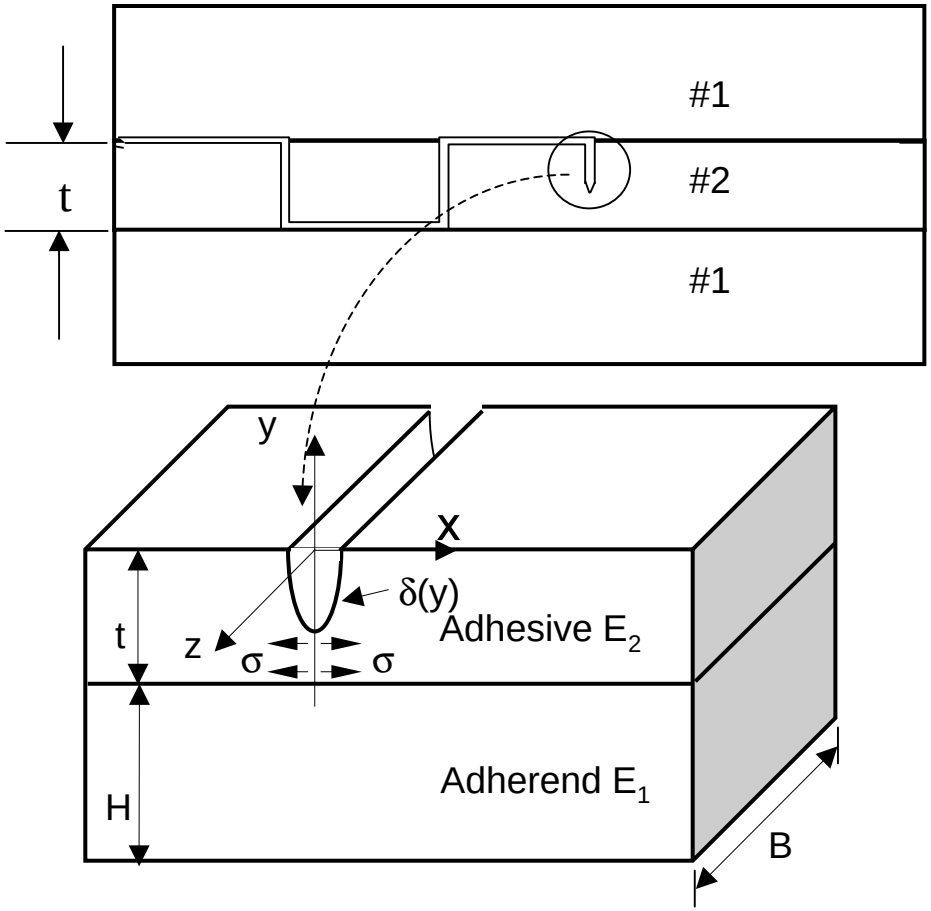

Fig. 5. The geometry and the stress state of a transverse crack in the DCB specimen with simplified crack trajectory for directionally unstable crack propagation.

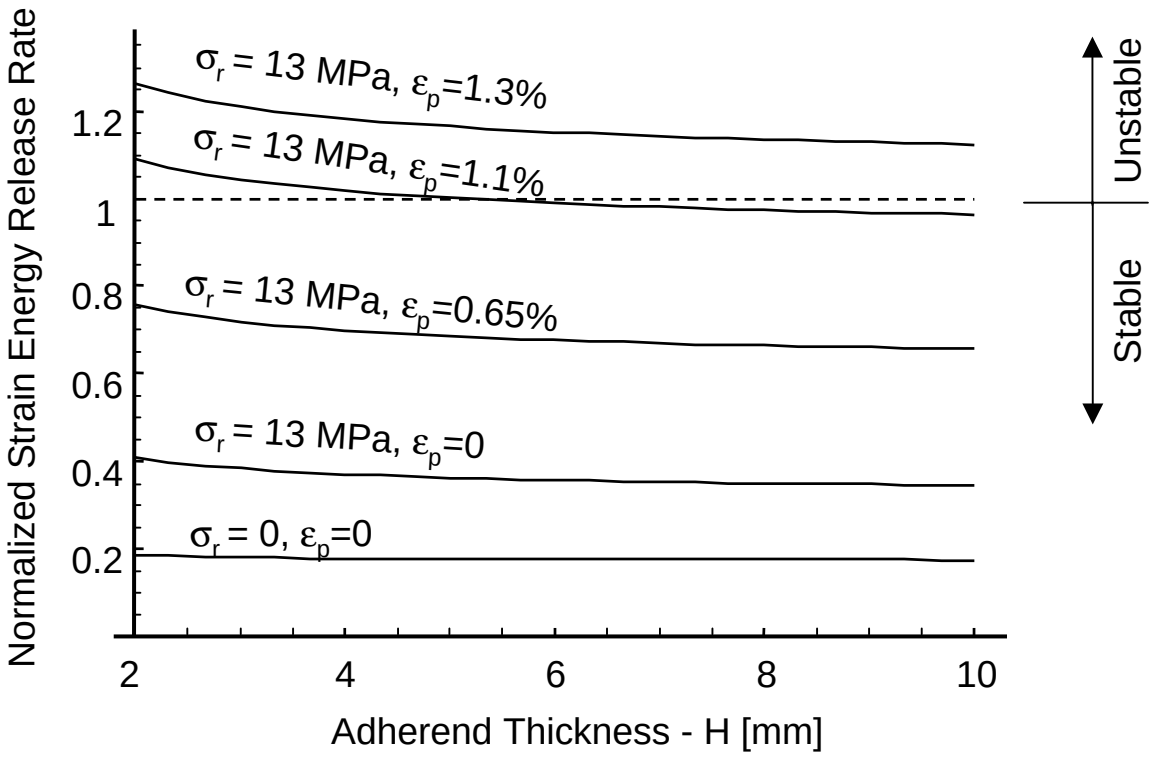

Fig. 6. Available strain energy release rate for directionally unstable crack propagation in DCB specimen with various conditions.

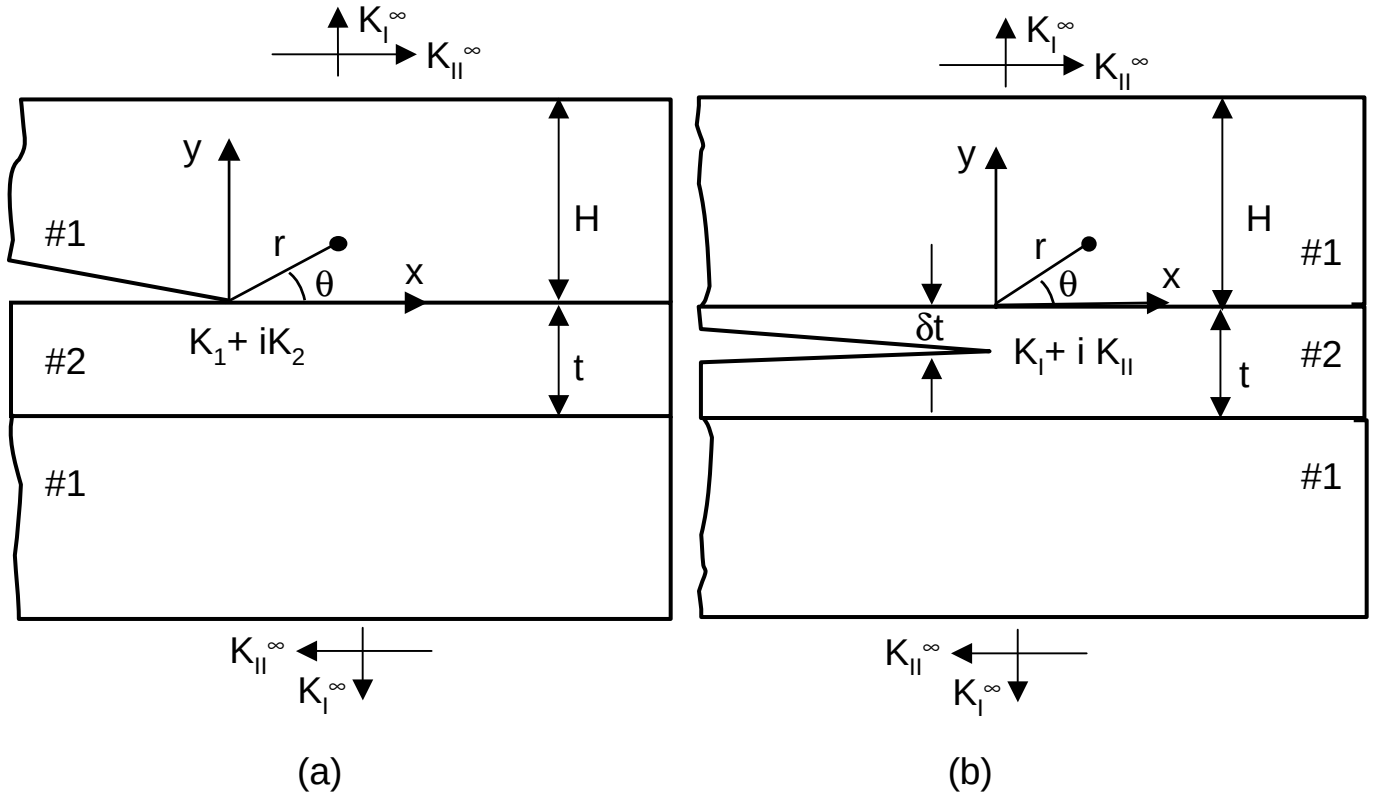

Fig. 7. Cracks in a DCB specimen: a) interfacial crack; b) cohesive crack. The specimen is under external K_I^∞, and K_{II}^∞ loading, which can also be described as far field stress intensity factors.

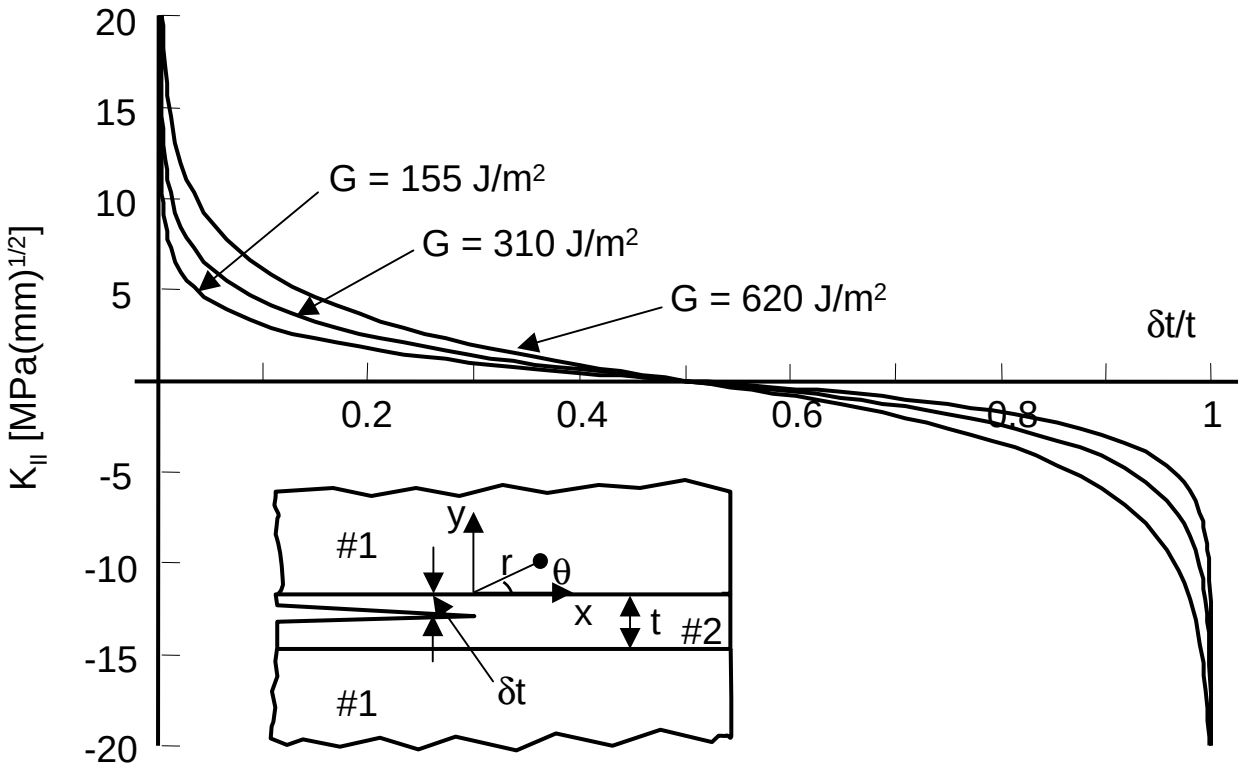

Fig. 8. The curve of local mode II stress intensity factor K_{II} versus the non-dimensional location of the sub-interfacial crack varies with the applied strain energy level.

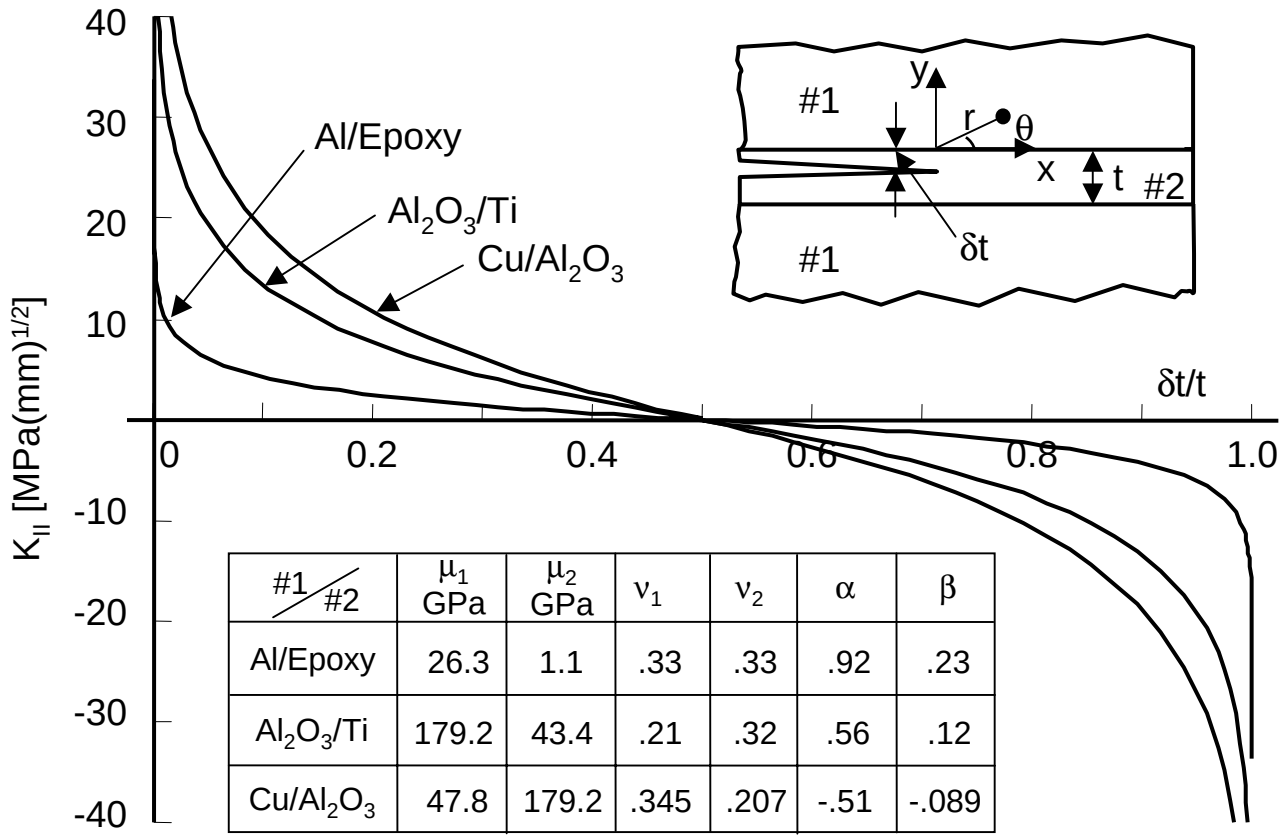

#1 / #2	μ_1 GPa	μ_2 GPa	ν_1	ν_2	α	β
Al/Epoxy	26.3	1.1	.33	.33	.92	.23
Al_2O_3/Ti	179.2	43.4	.21	.32	.56	.12
Cu/Al_2O_3	47.8	179.2	.345	.207	-.51	-.089

Fig. 9. Parametric study of the local mode II stress intensity factor K_{II} versus the non-dimensional location of the sub-interfacial crack for different material combinations.

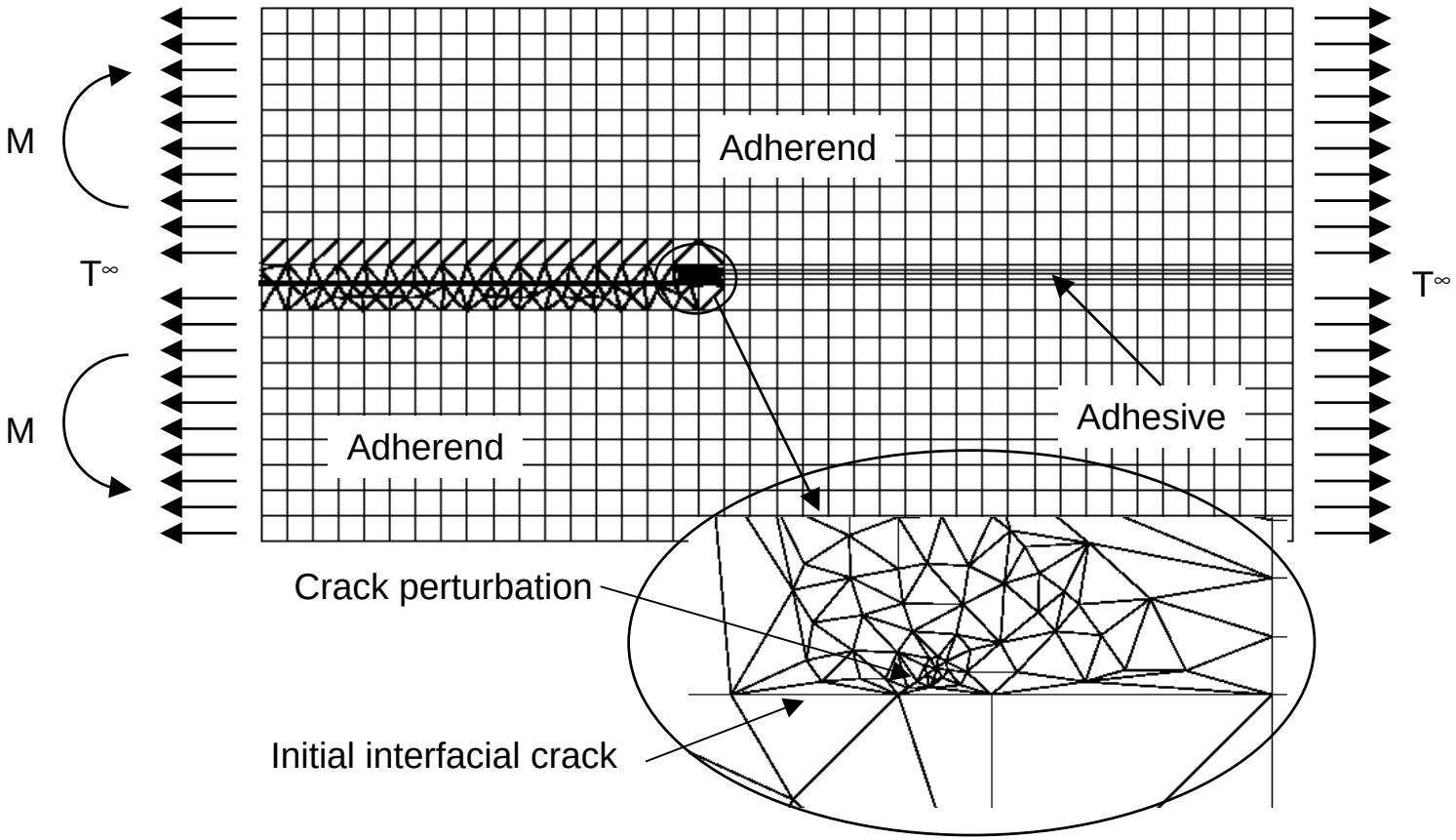

Fig. 10. The finite element mesh for predicting the crack trajectory in DCB specimen using Franc2dl.

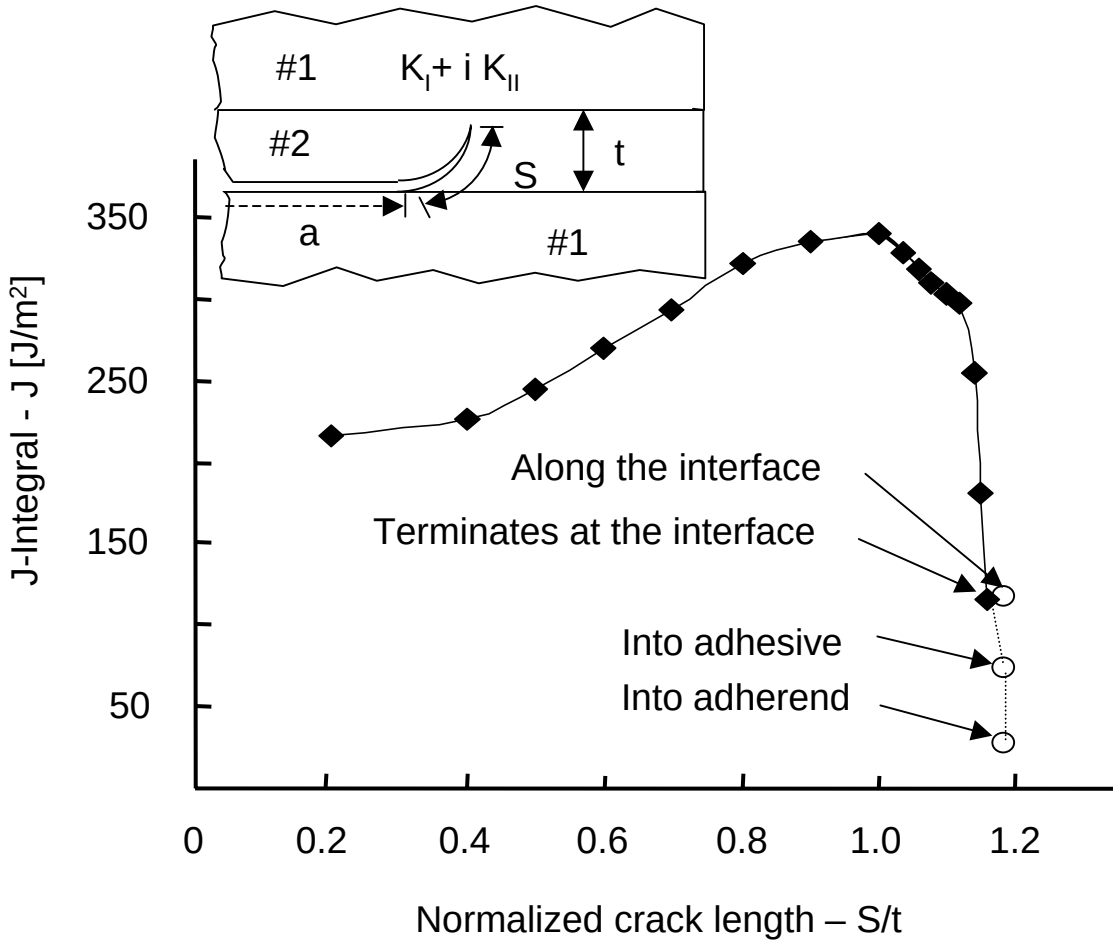

Fig. 11. Strain energy release rate (J-integral value) available at the crack tip versus the non-dimensional crack length obtained using the finite element analysis.

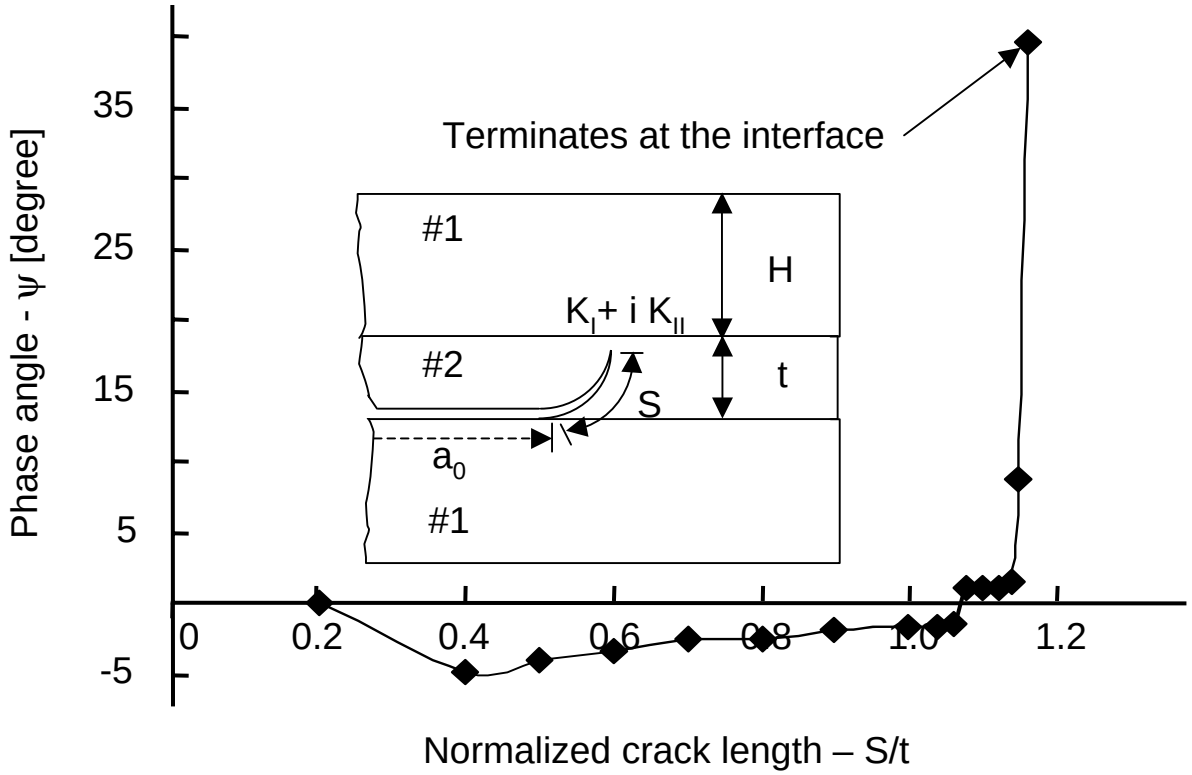

Fig. 12. Phase angle at the crack tip versus the non-dimensional crack length obtained by the finite element analysis.

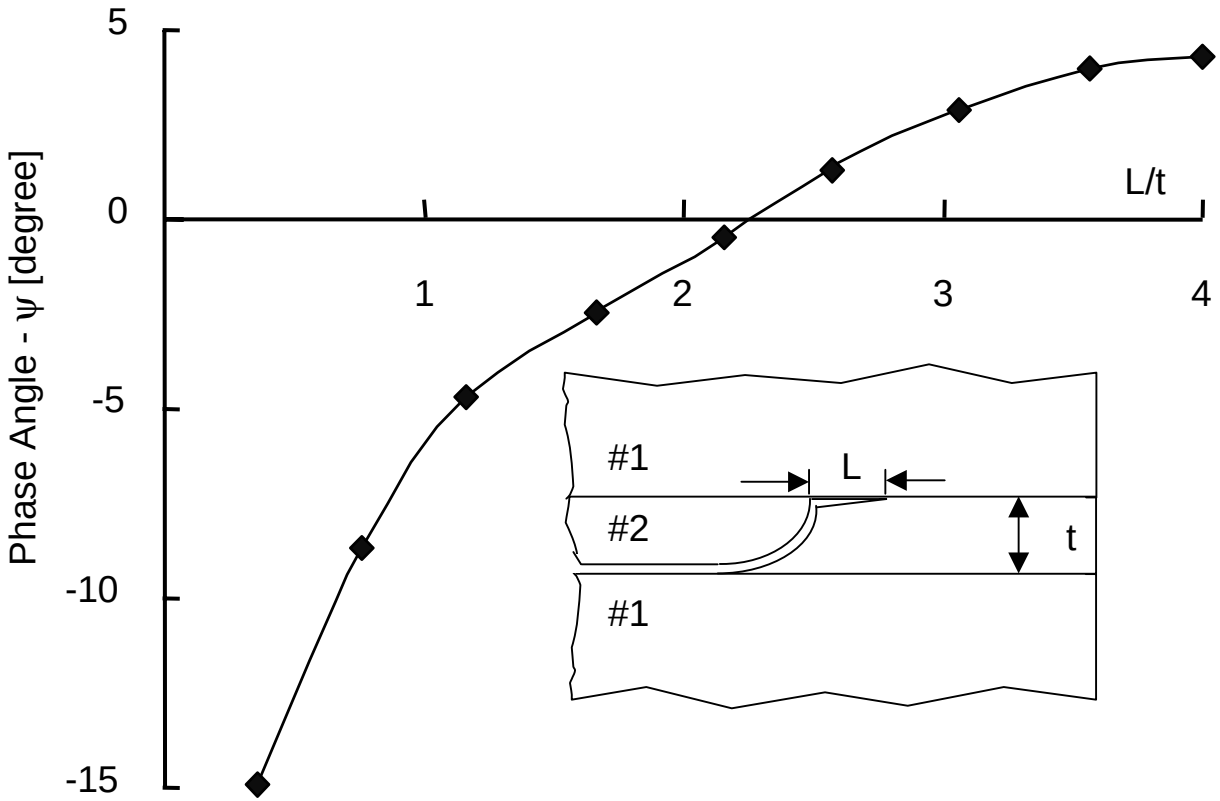

Fig. 13. Phase angle at the crack tip versus the non-dimensional interfacial crack length obtained by the finite element analysis.

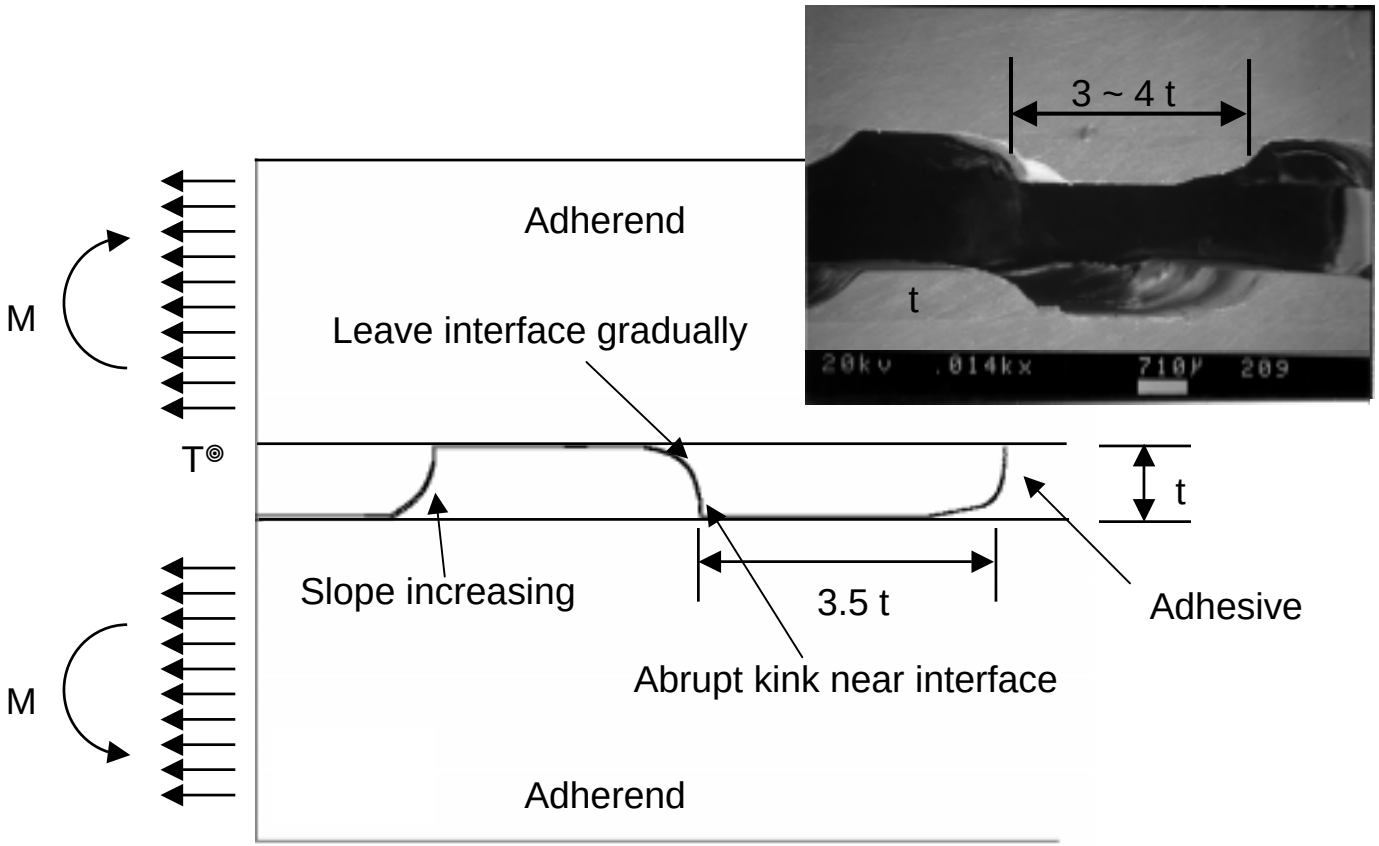

Fig. 14. The crack trajectory predicted by the finite element analysis using Franc2dl. The result reflects the overall characteristics of the actual crack trajectory such as the characteristic length of the crack as shown in the SEM micrograph.